Electronic Supplementary Material (ESI) for Physical Chemistry Chemical Physics.
This journal is © the Owner Societies 2015

1) Experimental methods

Samples of glucosamine 6-sulfate were obtained from Sigma Aldrich and used without further purification.

A. IRMPD experiments

Glucosamine 6-sulfate was prepared at a concentration of 250 µM in a water/methanol (50:50) solution for electrospraying.

Action IR spectroscopy was performed using a Thermo Finnigan LCQ 3D ion trap with an electrospray ionization source modified to allow injecting a laser beam. For the 700-1700 cm^{-1} region, the beamline of the Free Electron Laser for Infrared eXperiments (FELIX) was injected through a KRS-5 window into the ion trap of the mass spectrometer. Mass-selected ions were fragmented upon resonant IR excitation and the photofragmentation yield was plotted as a function of the wavenumber to obtain vibrational spectra. Each experiment was performed at a repetition rate of 10 Hz with a typical irradiation time of 400 ms.

B. NMR experiments

NMR spectra were recorded on Bruker AVANCE III 300 and AVANCE III 500 spectrometers at 300.13 MHz and 500.13 MHz, respectively for ^1H NMR. Chemical shifts (δ) are measured in parts per million (ppm) and were calibrated relatively to the residual signal of methanol (δ = 3.31 ppm).

Glucosamine 6-sulfate was dissolved in a CD_3OD/D_2O mixture (1:1). The two pyranoside anomers ratio (α or β) were monitored by integrating the H-2 signals (in red on Scheme SI XXX) on the NMR spectrum at 3.24 ppm for the α anomer and 2.95 ppm for the β anomer.

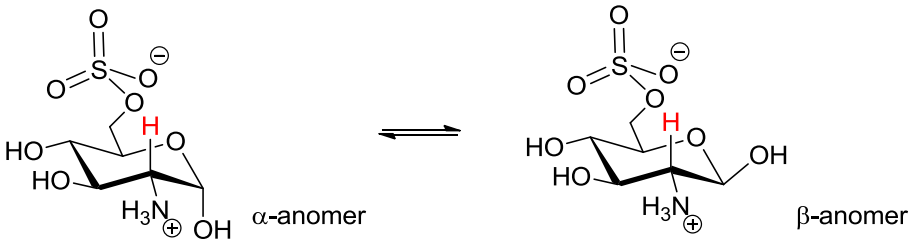

Scheme S1: equilibrium between the two pyranoside anomers of glucosamine 6-sulfate. H-2 protons used for the following of the equilibrium are indicated in red.

30 minutes after the sample preparation, the α anomer was found very predominant with α/β = 89:11 (see Figure S1)

After 16 hours at room temperature, the α/β ratio changed to α/β = 73:27 (see Figure S2)

We could say that in this conditions the equilibrium was attained in less than 16 hours since approximately the same α/β ratio was observed after 2 days, α/β = 74:26 (see Figure S3)

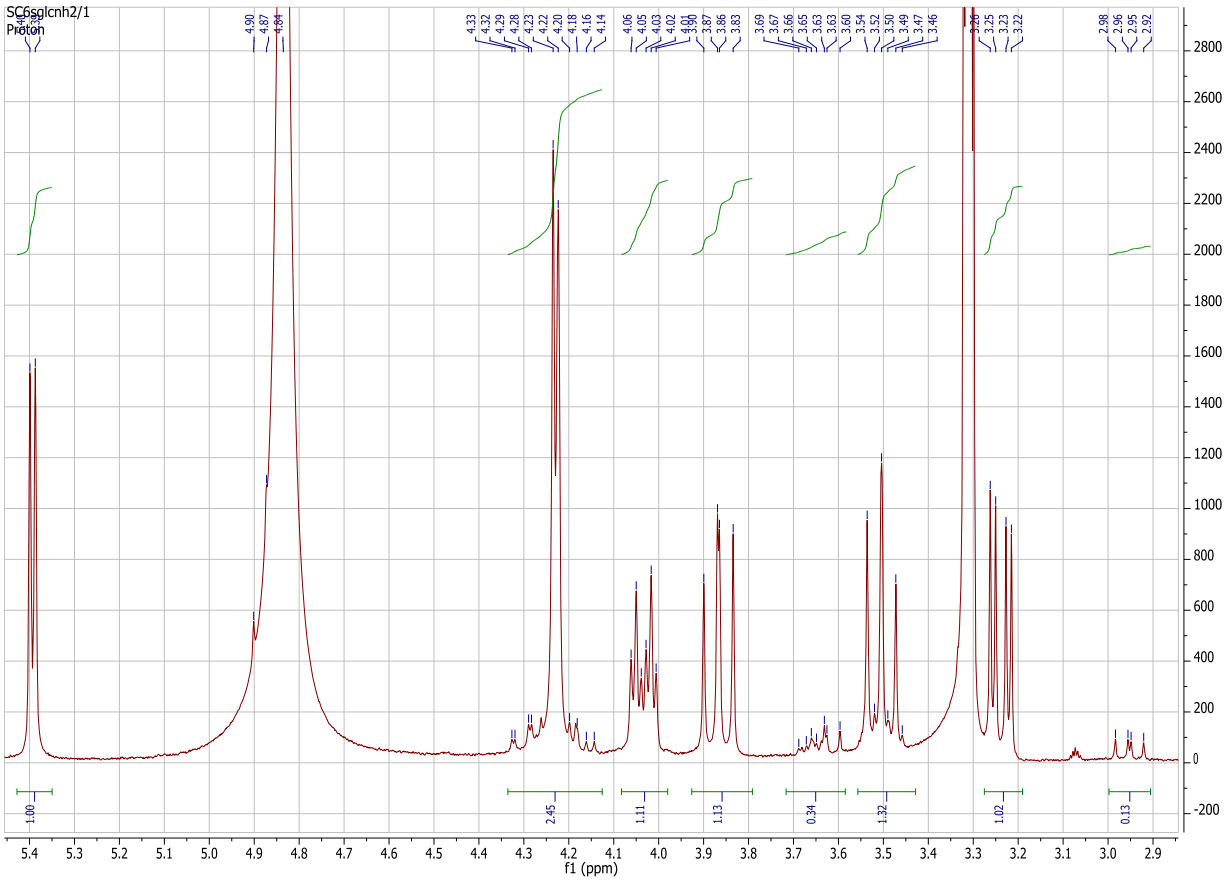

Figure S1: NMR spectrum of glucosamine 6-sulfate after 30 min.

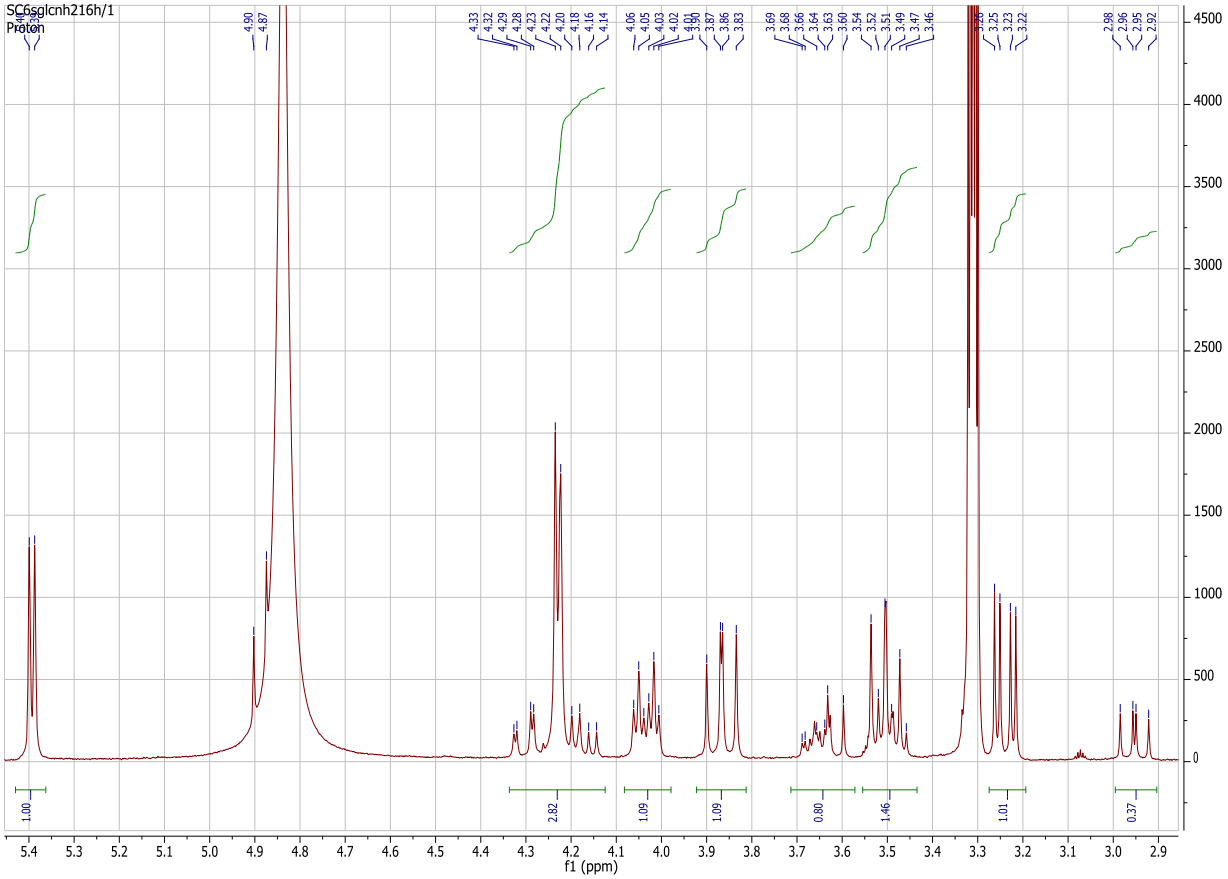

Figure S2: NMR spectrum of glucosamine 6-sulfate after 16 h.

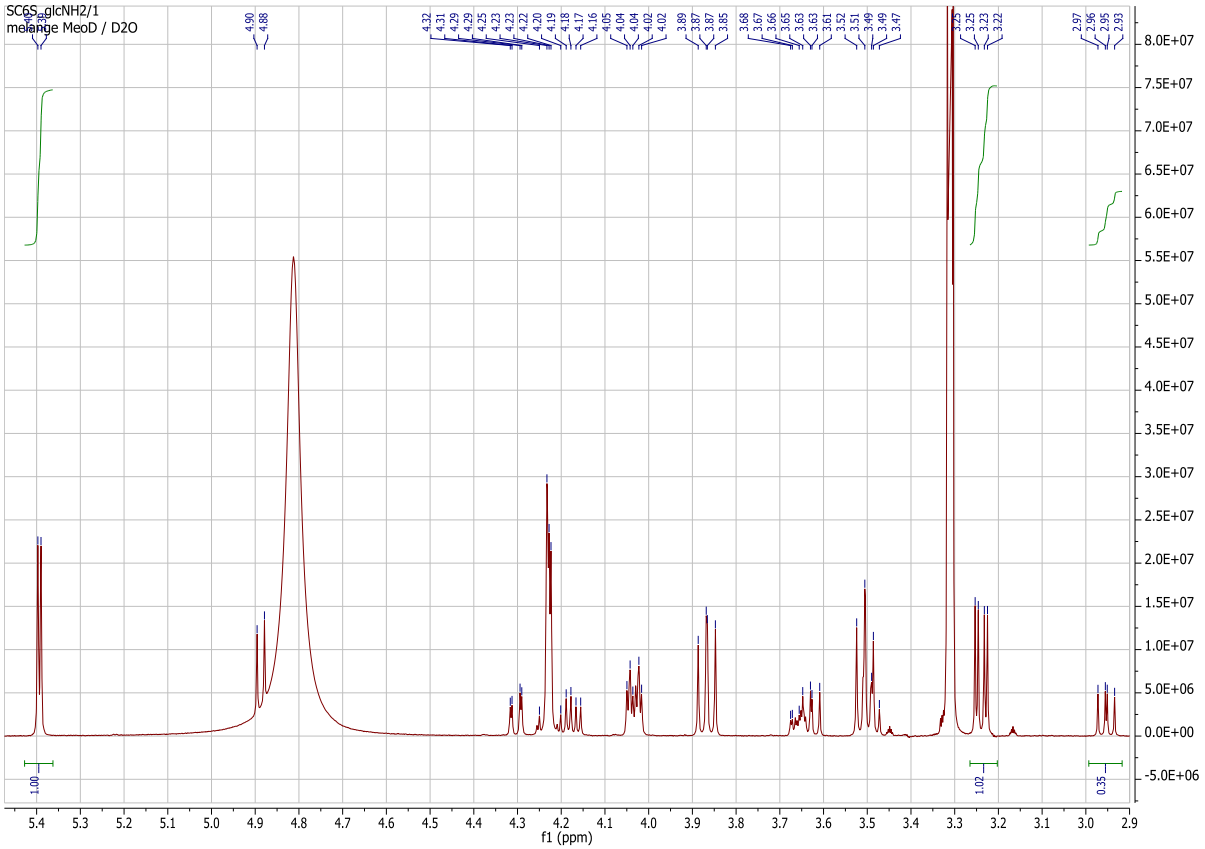

Figure S3: NMR spectrum of glucosamine 6-sulfate after 2 days (recorded at 500 MHz).

2) CPU time for dimethyl sulfate (4)

In the table S1, the C.P.U time (in hours) of all the functionals and basis sets are written for our biggest benchmark system, i.e. dimethyl sulfate (4), to give an idea of the computational cost of anharmonic calculations with different couples functional/basis.

	MP2	PBE0	M06-2X	LC-PBE	ω-B97XD	CAM-B3LYP	B3LYP	BLYP
SNSD	875	55	87	72	83	71	55	52
6-311+G(d)	361	26	43	33	36	32	26	28
6-311++G**	646	43	53	44	44	41	38	34
6-311++G(df,pd)	2334	119	141	178	176	171	104	93
6-311++G(2d,2pd)	4104	200	254	333	313	293	197	155
6-311++G(3df,3pd)	10848	298	368	470	505	489	307	238
cc-pVDZF12	1884	85	119	160	154	154	87	78
cc-pVDZ	193	17	24	17	18	17	20	14
cc-pVTZ	3340	119	159	210	221	201	138	109
cc-pVQZ		1672	1613	2307	2284	2144	1509	1049
Aug-cc-pVTZ		454	762	824	819	1441	450	361

Table S1: C.P.U. time (hours) for $DMSO_4$

3) Vibrational frequencies of the benchmark species

We chose to write down the frequencies and their variation for one of the five method or functional that gives good results at the harmonic level with re-optimized scaling factors, here it is CAM-B3LYP with the basis 6-311++G(2df,2pd). We also put in the four following tables the results of anharmonic calculations of CAM-B3LYP, PBE0 and M06-2X with the same basis. It allows direct comparison with harmonic computation for CAM-B3LYP. It shows one case that does not work when investigating anharmonic effects whereas it worked quite well at harmonic level, i.e. M06-2X.

Finally, the frequencies and their errors obtained with the hybrid GVPT2 method are shown in the tables for both CAM-B3LYP and PBE0.

Table S2: Vibrational frequencies for SO_2, $(H_2O)_2$, $HSO_4^-\cdot H_2O$

	M06-2X/6-311++G(2df,2pd) anharm.	PBE0/6-311++G(2df,2pd) anharm.	PBE0/hybrid GVPT2	CAM-B3LYP/hybrid GVPT2	CAM-B3LYP/6-311++G(2df,2pd) scaled	CAM-B3LYP/6-311++G(2df,2pd) anharm.	Experiment
SO_2							
SO_2 scissoring	539	526	526	531	520	530	518
SO_2 stretching sym	1230	1193	1195	1209	1189	1207	1151
SO_2 stretching asym	1425	1386	1388	1399	1377	1397	1362
$(H_2O)_2$							
OH (H bond) bend	340	506	470	502	642	515	523
H_2O stretch sym (H bond)	3283	3560	3594	3584	3559	3580	3601
H_2O stretch asym (H bond)	3268	3770	3782	3758	3747	3745	3735
H_2O stretch asym	4124	3792	3785	3766	3762	3751	3745
$HSO_4^-\cdot H_2O$							
SO-(H) stretch	815	748	744	748	770	756	752
SO_3 stretch sym	1056	1040	1041	1041	1030	1042	1049
(S)OH bend + SO stretch	1138	1178	1186	1188	1200	1191	1193
SO_2 stretch asym	1417	1209	1209	1207	1191	1207	1218
(S)OH bend + SO stretch	1294	1309	1316	1313	1307	1308	1309
H_2O scissoring	1744	1684	1679	1676	1657	1682	1677

Table S3: Vibrational frequencies for $DMSO$, $DMSO_2$, $DMSO_4$

	M06-2X/6-311++G(2df,2pd) anharm.	PBE0/6-311++G(2df,2pd) anharm.	PBE0/hybrid GVPT2	CAM-B3LYP/hybrid GVPT2	CAM-B3LYP/6-311++G(2df,2pd) scaled	CAM-B3LYP/6-311++G(2df,2pd) anharm.	Experiment
DMSO							
CSC stretch asym	661	682	682	686	684	686	670
S=O stretch	1093	1115	1114	1110	1098	1110	1100
Double CH_3 resp	3273	2942	2939	2954	2922	2958	2928
Double CH_2 stretch asym	3330	3020	3017	3021	3016	3025	2998
$DMSO_2$							
SO_2 wagg	429	456	454	464	450	464	468
SO_2 scissoring	485	486	487	494	482	491	494
CSC stretch sym	680	679	679	684	678	682	682
CSC stretch asym	693	737	736	747	739	745	746
CH_3	836	924	922	943	930	944	934
SO_2 sym	1160	1160	1161	1165	1153	1163	1160
SO_2 stretch asym	1361	1312	1352	1329	1317	1347	1358
$DMSO_4$							
SO_2(Me) stretch sym	776	750	753	756	750	755	758
SO_2(Me) stretch asym	828	811	814	816	809	815	814
CO_2 stretch (sym et asym)	1051	1030	1031	1030	1035	1028	1006
SO_2 (O=S=O) stretch sym	1232	1201	1209	1182	1199	1211	1206
SO_2 (O=S=O) stretch asym	1442	1415	1419	1421	1410	1419	1410

Table S4: Difference between experiment and calculations for SO_2, $(H_2O)_2$, $HSO_4^-\cdot H_2O$

	M06-2X/6-311++G(2df,2pd) anharm.	PBE0/6-311++G(2df,2pd) anharm.	PBE0/hybrid GVPT2	CAM-B3LYP/hybrid GVPT2	CAM-B3LYP/6-311++G(2df,2pd) scaled	CAM-B3LYP/6-311++G(2df,2pd) anharm.	Experiment
SO_2							
SO_2 scissoring	20.8	7.9	8.3	12,6	2.4	12,4	518
SO_2 stretching sym	79.4	41.9	43.7	57,5	38.3	56,3	1151
SO_2 stretching asym	62.5	23.8	26.2	36,5	15.2	34,9	1362
$(H_2O)_2$							
OH (H bond) bend	-183	-16.5	-52.9	-21,2	119.4	-8,0	523
H_2O stretch sym (H bond)	-317	-11.2	-6.9	-17,0	-42,2	-20,7	3601
H_2O stretch asym (H bond)	-466	35	46.8	23,3	11,5	9,6	3735
H_2O stretch asym	379	47.4	40	20,6	16,5	5,9	3745
$HSO_4^-\cdot H_2O$							
SO-(H) stretch	63.3	-3.5	-8.2	-3,9	17,9	4,1	752
SO_3 stretch sym	7.3	-9.4	-8.3	-8,2	-18.6	-6,6	1049
(S)OH bend + SO stretch	-54.9	-15.1	-6.6	-4,8	7.0	-2,4	1193
SO_2 stretch asym	-1.3	-8.6	-8.6	-10,8	-26.7	-10,7	1218
(S)OH bend + SO stretch	-14.8	0.1	6.8	3,6	-1.8	-0,9	1309
H_2O scissoring	67.8	7.2	1.7	-1,0	-20.4	5,4	1677

Table S5: Difference between experiment and calculations for DMSO, $DMSO_2$, $DMSO_4$

	M06-2X/6-311++G(2df,2pd) anharm.	PBE0/6-311++G(2df,2pd) anharm.	PBE0/hybrid GVPT2	CAM-B3LYP/hybrid GVPT2	CAM-B3LYP/6-311++G(2df,2pd) scaled	CAM-B3LYP/6-311++G(2df,2pd) anharm.	Experiment
DMSO							
CSC stretch asym	-8.6	12.2	12.5	15,8	14.4	15,8	670
S=O stretch	-7	15.2	14.6	9,7	-2.2	9,8	1100
Double CH_3 resp	345	14.3	11.1	25,9	-5,9	29,5	2928
Double CH_2 stretch asym	331	21.9	18.9	23,2	17,9	26,7	2998
$DMSO_2$							
SO_2 wagg	-39.4	-11.9	-13.5	-3,6	-17.9	-4,3	468
SO_2 scissoring	-8.8	-7.8	-7.3	0,4	-11.5	-2,6	494
CSC stretch sym	-1.7	-2.6	-2.8	2,1	-3.8	-0,3	682
CSC stretch asym	-53.5	-.9.1	-9.6	0,7	-6.5	-1,2	746
CH_3	-97.7	-9.3	-12.5	9,4	-4.1	10,2	934
SO_2 sym	-0.4	0.1	1.4	5,1	-7.3	2,7	1160
SO_2 stretch asym	2.9	-46.3	-5.8	-29,4	-40.6	-11,3	1358
$DMSO_4$							
SO_2(Me) stretch sym	18.3	-8	-5.2	-1,8	-7.9	-3,1	758
SO_2(Me) stretch asym	13.6	-2.7	-0.4	2,3	-4.7	0,8	814
CO_2 stretch (sym et asym)	45.5	23.5	3.3	24,1	28.7	22,2	1006
SO_2 (O=S=O) stretch sym	25.6	4.6	9.3	6.7	-6.5	4.7	1206
SO_2 (O=S=O) stretch asym	32.5	5.1	24.9	11.2	-0.4	9.4	1410

4) Geometry of the benchmark species (DFT CAM-B3LYP/6-311++G(2df,2pd))

The geometries were optimized using Gaussian 09 with the following options :

#SCF=(XQC,Tight) Opt(Tight)

Here, you can find the optimized geometries with CAM-B3LYP/6-311++G(2df,2pd) for all of our benchmark species . The coordinates are in Angstrom.

$DMSO_4$:

C	6	1.585843	-1.142206	-1.135153
O	8	1.226004	0.065345	-0.441286
S	16	0.000000	0.000000	0.552255
O	8	0.000000	1.247654	1.231579
C	6	-1.585843	1.142206	-1.135153
O	8	-1.226004	-0.065345	-0.441286
O	8	0.000000	-1.247654	1.231579
H	1	-2.454670	0.880826	-1.728707
H	1	-0.770757	1.463745	-1.780192
H	1	-1.829839	1.922424	-0.420568
H	1	0.770757	-1.463745	-1.780192
H	1	1.829839	-1.922424	-0.420568
H	1	2.454670	-0.880826	-1.728707

$DMSO_2$:

S	16	0.000000	0.000000	0.185854
O	8	-1.249084	0.000000	0.905295
C	6	0.000000	-1.402118	-0.906326
H	1	-0.898977	-1.387994	-1.515386
H	1	0.000000	-2.276505	-0.260468
O	8	1.249084	0.000000	0.905295
C	6	0.000000	1.402118	-0.906326

H	1	0.898977	1.387994	-1.515386
H	1	0.000000	2.276505	-0.260468
H	1	-0.898977	1.387994	-1.515386
H	1	0.898977	-1.387994	-1.515386

DMSO:

C	6	-0.257096	-0.773634	1.348526
S	16	-0.257096	0.424106	0.000000
O	8	1.089438	1.056239	0.000000
H	1	0.621119	-1.409033	1.255054
H	1	-0.206154	-0.206697	2.274054
H	1	-1.173369	-1.360272	1.323907
C	6	-0.257096	-0.773634	-1.348526
H	1	0.621119	-1.409033	-1.255054
H	1	-0.206154	-0.206697	-2.274054
H	1	-1.173369	-1.360272	-1.323907

$HSO_4^- \cdot H_2O$:

S	16	-0.564726	-0.108715	0.000013
O	8	-2.003367	-0.024344	0.000025
O	8	-0.097734	1.460369	-0.000084
O	8	0.034715	-0.663658	-1.213729
H	1	0.871303	1.441204	-0.000094
O	8	2.547305	0.009161	-0.000031
H	1	2.019513	-0.322891	0.743489
O	8	0.034743	-0.663516	1.213806
H	1	2.019495	-0.322978	-0.743499

SO_2:

S	16	0.000000	0.000000	0.365014
O	8	0.000000	1.231533	-0.365014
O	8	0.000000	-1.231533	-0.365014

$(H_2O)_2$:

O	8	-0.001612	-1.375160	0.000000
H	1	-0.475480	-1.706077	0.766897
O	8	-0.001612	1.503519	0.000000
H	1	0.083202	0.539727	0.000000
H	1	0.893553	1.845555	0.000000
H	1	-0.475480	-1.706077	-0.766897

5) Vibrational spectra of the benchmark species

Detail on the hybrid approach

The idea is to sum the harmonic frequencies given by CAM-B3LYP/6-311++G(2df,2pd) (instead of those calculated with 6-311++G**) with the anharmonic corrections computed with the basis 6-311++G** to obtain the anharmonic frequencies. Because the normal modes of the two basis sets might not be in the same order, we need to associate correctly the normal modes of a basis with those of the other basis.

The geometry should be the same when optimized with the lower and the bigger basis set. Any change in the geometry could lead to different normal modes. In this situation, the association between the modes of the two basis sets becomes impossible and the hybrid GVPT2 method cannot be used.

We developed a C++ program to make the link between modes calculated with the two different basis sets. If you interested in this program, you can acquire it by sending a message at abdul-rahman.allouche@univ-lyon1.fr or loic.barnes@univ-lyon1.fr

In the following figures, we show the spectra obtained with the methods cited in section 3. When the data of experimental spectra were not available we draw only the experimental frequencies.

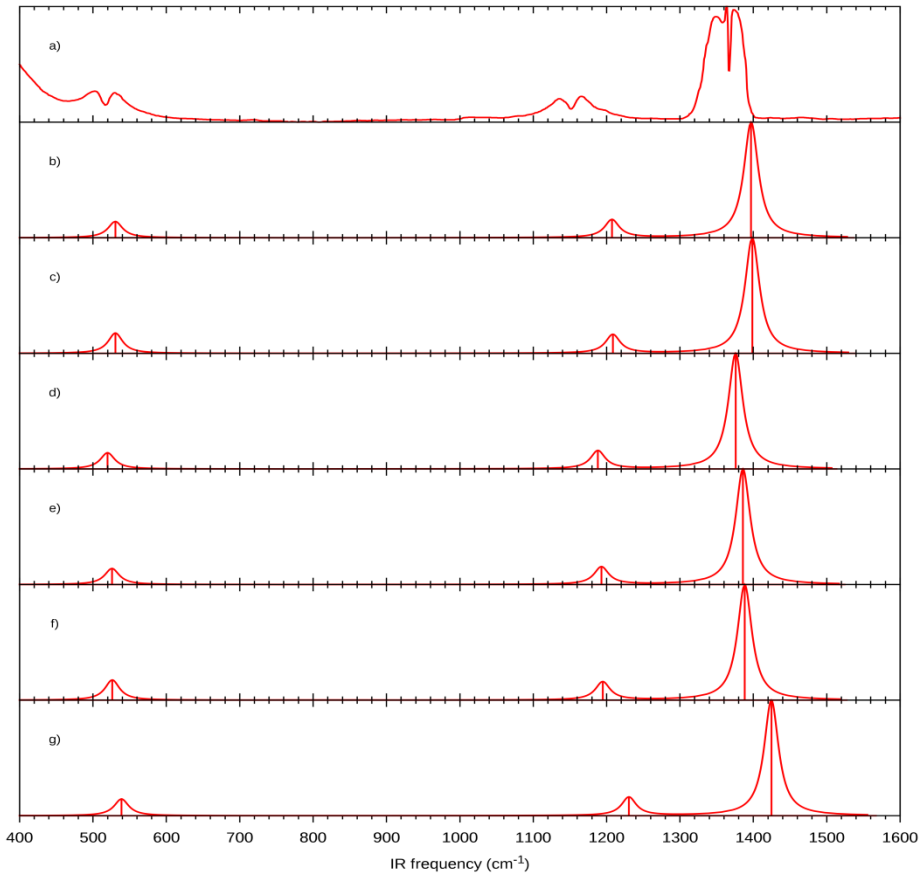

Figure S4: IR spectra of SO_2 a) experimental spectrum from NIST b) GVPT2 CAM-B3LYP/6-311++G(2df,2pd) c) GVPT2 CAM-B3LYP/hybrid d) CAM-B3LYP/6-311++G(2df,2pd) harmonic scaled e) GVPT2 PBE0/6-311++G(2df,2pd) f) GVPT2 PBE0/hybrid g) GVPT2 M06-2X/6-311++G(2df,2pd)

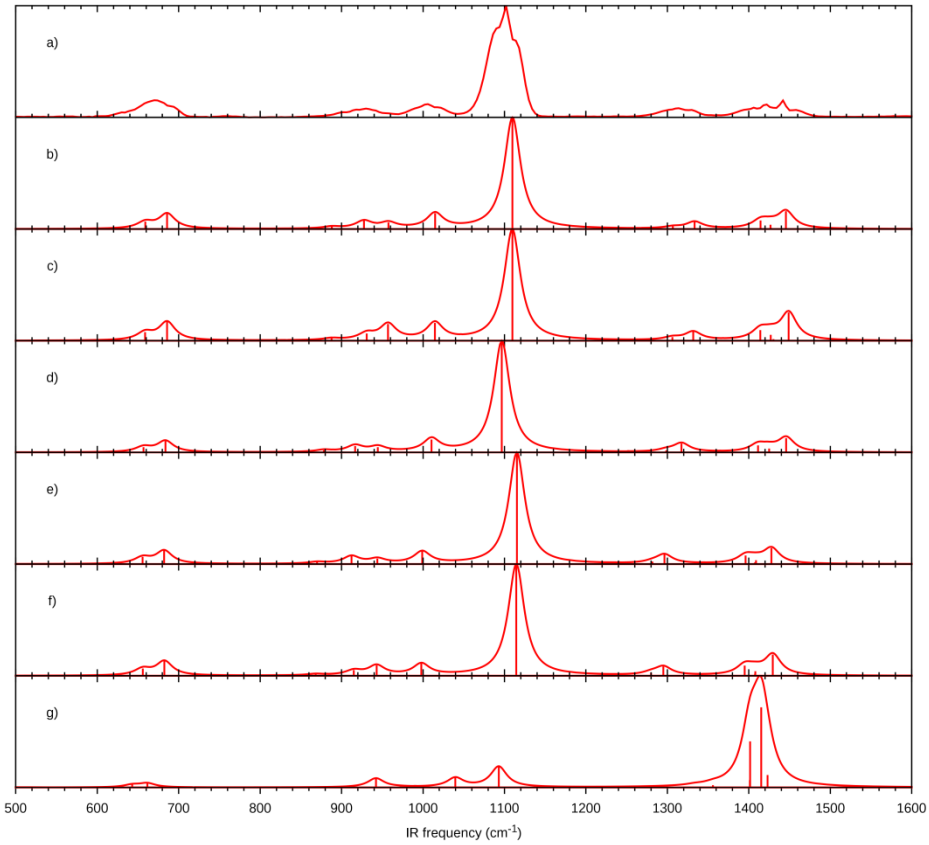

Figure S5: IR spectra of DMSO a) experimental spectrum from NIST b) GVPT2 CAM-B3LYP/6-311++G(2df,2pd) c) GVPT2 CAM-B3LYP/Hybrid d) CAM-B3LYP/6-311++G(2df,2pd) harmonic scaled e) GVPT2 PBE0/6-311++G(2df,2pd) f) GVPT2 PBE0/hybrid g) GVPT2 M06-2X/6-311++G(2df,2pd)

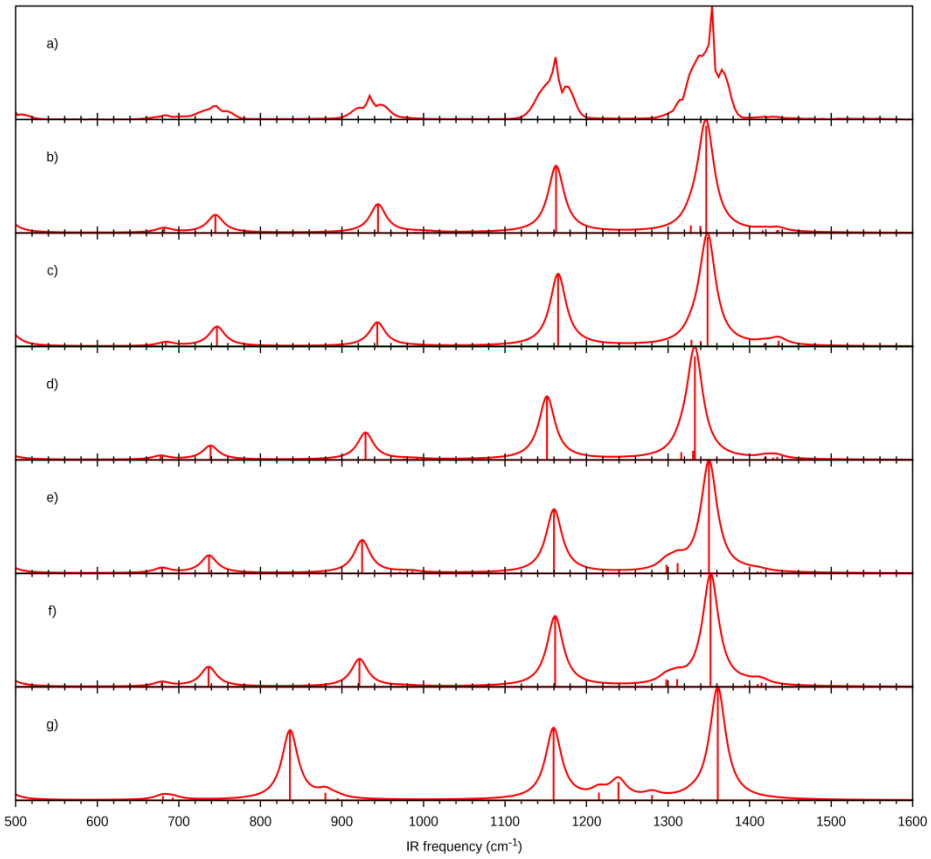

Figure S6: IR spectra of $DMSO_2$ a) experimental spectrum from NIST b) GVPT2 CAM-B3LYP/6-311++G(2df,2pd) c) GVPT2 CAM-B3LYP/Hybrid d) CAM-B3LYP/6-311++G(2df,2pd) harmonic scaled e) GVPT2 PBE0/6-311++G(2df,2pd) f) GVPT2 PBE0/hybrid g) GVPT2 M06-2X/6-311++G(2df,2pd)

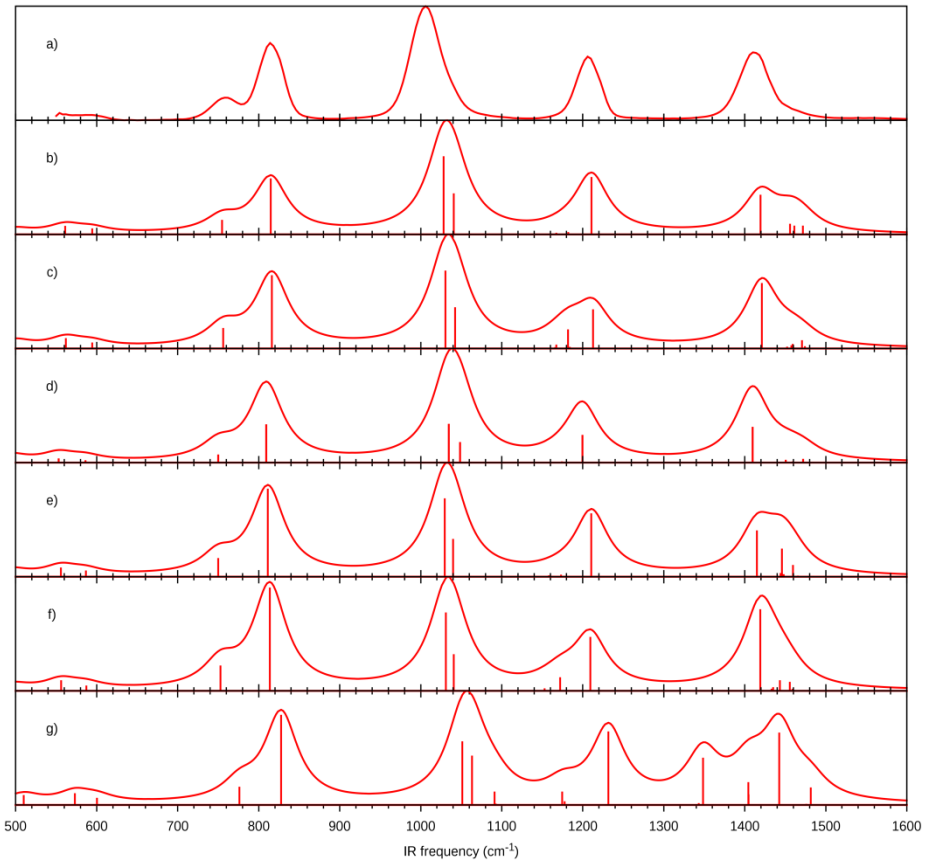

Figure S7: IR spectra of $DMSO_4$ a) experimental spectrum from NIST b) GVPT2 CAM-B3LYP/6-311++G(2df,2pd) c) GVPT2 CAM-B3LYP/Hybrid d) CAM-B3LYP/6-311++G(2df,2pd) harmonic scaled e) GVPT2 PBE0/6-311++G(2df,2pd) f) GVPT2 PBE0/hybrid g) GVPT2 M06-2X/6-311++G(2df,2pd)

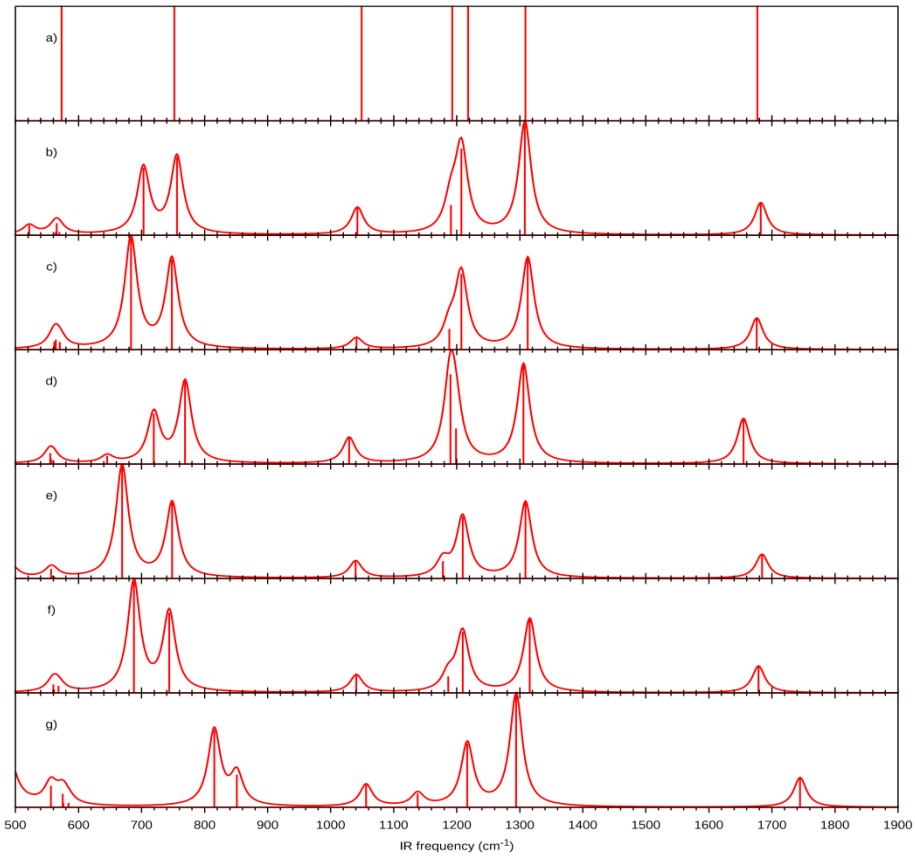

Figure S8: IR spectra of $HSO_4^-\cdot H_2O$ a) experimental frequencies from Ref : ESI, T. I. Yacovitch, T. Wende, L. Jiang, N. Heine, G. Meijer, D. M. Neumark and K. R. Asmis, J. Phys. Chem. Lett. 2, 2135-2140 (2011). b) GVPT2 CAM-B3LYP/6-311++G(2df,2pd) c) GVPT2 CAM-B3LYP/Hybrid d) CAM-B3LYP/6-311++G(2df,2pd) harmonic scaled e) GVPT2 MP2/6-311++G(2df,2pd) f) MP2/6-311++G(2df,2pd) harmonic scaled

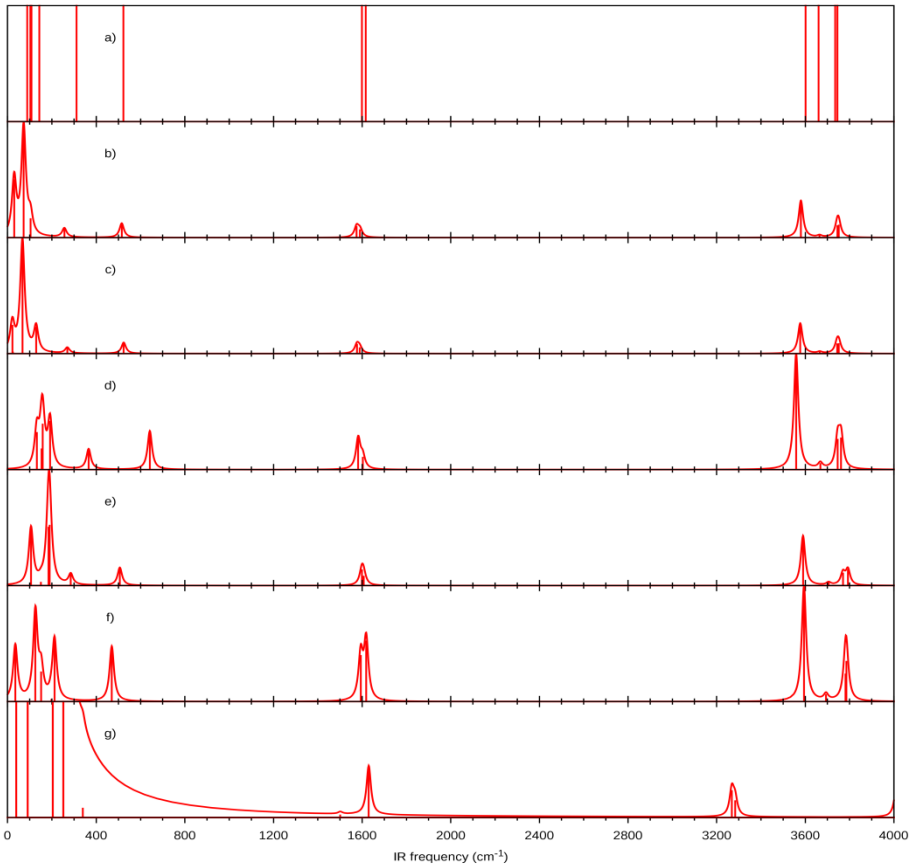

Figure S9: IR spectra of $(H_2O)_2$ a) experimental frequencies from Ref : R. Kalescky, W. Zou, E. Kraka and D. Cremer, Chemical Physics Letters, 554 (2012) 243-247 b) GVPT2 CAM-B3LYP/6-311++G(2df,2pd) c) GVPT2 CAM-B3LYP/Hybrid d) CAM-B3LYP/6-311++G(2df,2pd) harmonic scaled e) GVPT2 PBE0/6-311++G(2df,2pd) f) GVPT2 PBE0/hybrid g) GVPT2 M06-2X/6-311++G(2df,2pd)

6) Anharmonic PBE0 spectrum of dimethyl sulfate (4)

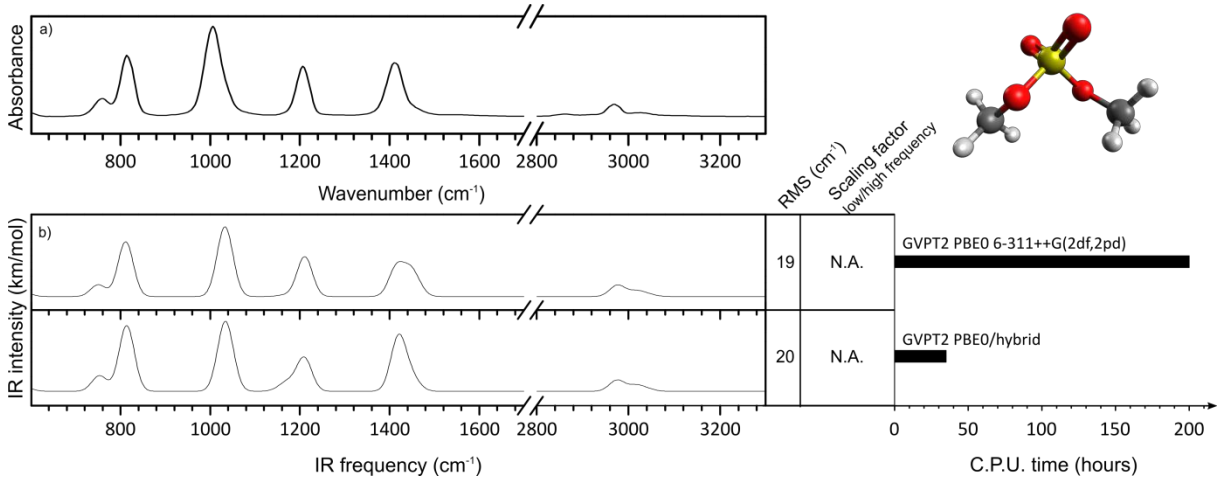

Figure S10: IR spectra of dimethyl sulfate (4) a) experimental spectrum from NIST; b) convoluted anharmonic spectra

7) Application to glucosamine 6-phosphate

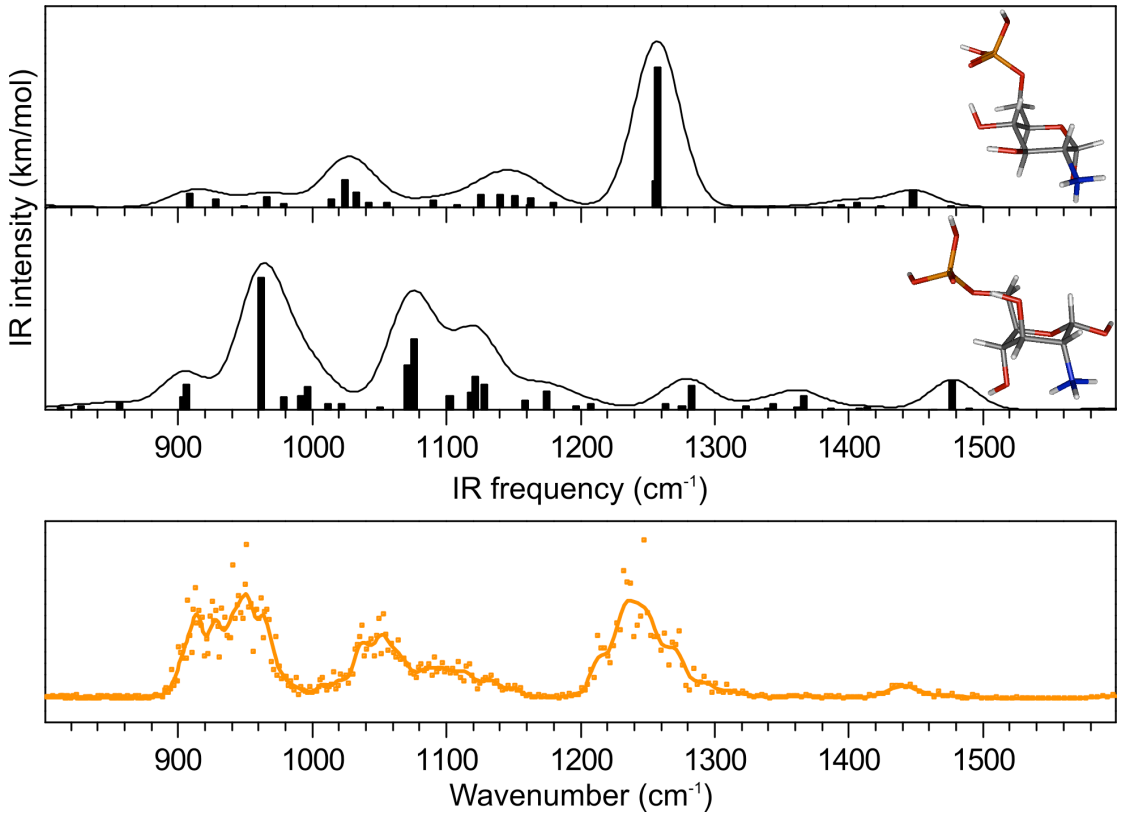

Fig. S11: Fingerprint IR spectra of glucosamine 6-phosphate. Top panel: CAM-B3LYP/ hybrid spectra of the two lowest energy structures; Lower panel: IR-MPD spectrum.

With two broad dominant features around 940 cm-1 and 1250 cm-1, the IR-MPD spectrum of glucosamine 6-phosphate is distinct from the IR-MPD spectrum of the isobaric species glucosamine 6-sulfate.

The hybrid anharmonic spectra of the two lowest energy structures (a $^4C_1$ chair stabilized by a phosphate-OH(4) H-bond; and a $^1C_4$ chair stabilized by a phosphate-OH(3) H-bond) are shown in the top panel. Together, they account for the experimental spectrum: the intense feature centered around 1250 cm^{-1} corresponds to the P=O stretching vibration of the $^4C_1$ form, while the intense feature centered around 940 cm^{-1} corresponds to the phosphate OH bending vibration of the $^1C_4$ form.